ADVANCED FUNCTIONAL MATERIALS
www.afm-journal.de

Sustained-Release Synthetic Biomarkers for Monitoring Thrombosis and Inflammation Using Point-of-Care Compatible Readouts

*Jaideep S. Dudani, Colin G. Buss, Reid T. K. Akana, Gabriel A. Kwong, and Sangeeta N. Bhatia**

Postoperative infection and thromboembolism represent significant sources of morbidity and mortality but cannot be easily tracked after hospital discharge. Therefore, a molecular test that could be performed at home would significantly impact disease management. The laboratory has previously developed intravenously delivered "synthetic biomarkers" that respond to dysregulated proteases to produce a urinary signal. These assays, however, have been limited to chronic diseases or acute diseases initiated at the time of diagnostic administration. Here, a subcutaneously administered sustained-release system, using small poly(ethylene glycol) scaffolds (<10 nm) to promote diffusion into the bloodstream over a day, is formulated. The utility of a thrombin sensor to identify thrombosis and an Matrix metalloproteinase (MMP) sensor to measure inflammation is demonstrated. Finally, a companion paper ELISA (Enzyme-linked immunosorbent sssay), using printed wax barriers, with nanomolar sensitivity for urinary reporters for point-of-care detection is developed. The approach for subcutaneous delivery of nanosensors combined with urinary paper analysis may enable facile monitoring of at-risk patients.

1. Introduction

Postoperative patients are temporarily at an increased risk for complications that include infection and thrombosis, which can initiate without overt symptoms and be immediately life threatening after onset.[1–5] At the hospital, patients are closely monitored for clinical signs of complications in order to enable rapid, specific intervention. These tests include surveying for circulating levels of prothrombin fragment 1.2 and D-dimer, which serve as indicators of thrombosis or genetic tests for pathogenic infections.[6,7] By contrast, the primary method for monitoring after hospital discharge is patient education for the potential symptoms of common complications.[8] Therefore, the ability to clinically monitor at-risk patients after discharge with a molecular test has the potential to significantly decrease morbidity, mortality, and the cost of such complications. These diagnostics need to be simple, rapid, and noninvasive to enable patients to self-monitor and immediately identify if they need to return to a hospital. This category of monitoring options is currently unavailable for postoperative patients who have been discharged from clinical settings.

Recently, our laboratory developed molecular tests based on engineered readouts, or "synthetic biomarkers," which enable urinary monitoring of disease status by measuring local,

J. S. Dudani, C. G. Buss, R. T. K. Akana, G. A. Kwong,[+] S. N. Bhatia
Koch Institute for Integrative Cancer Research
Massachusetts Institute of Technology
Cambridge, MA 02139, USA
E-mail: sbhatia@mit.edu
J. S. Dudani, R. T. K. Akana
Department of Biological Engineering
Massachusetts Institute of Technology
Cambridge, MA 02139, USA
C. G. Buss, G. A. Kwong, S. N. Bhatia
Institute for Medical Engineering and Science
Massachusetts Institute of Technology
Cambridge, MA 02139, USA
S. N. Bhatia
Electrical Engineering and Computer Science
Massachusetts Institute of Technology
Cambridge, MA 02139, USA

DOI: 10.1002/adfm.201505142

S. N. Bhatia
Department of Medicine
Brigham and Women's Hospital and Harvard Medical School
Boston, MA 02115, USA
S. N. Bhatia
Broad Institute of Massachusetts Institute of Technology and Harvard
Cambridge, MA 02139, USA
S. N. Bhatia
Howard Hughes Medical Institute
Cambridge, MA 02139, USA
[+]Present address: Wallace H. Coulter Department of Biomedical Engineering, Georgia Tech and Emory School of Medicine, Atlanta, GA 30332, USA

defined protease activity such as thrombin in blood clots.[9–12] These synthetic biomarkers offer an opportunity to monitor at-risk patients noninvasively through the urine with a range of analytical techniques including mass spectrometry[9] and LFA paper strips[11] to quantify urinary reporters. For these previous iterations, we tethered protease-cleavable peptides to iron oxide particles and delivered the resulting nanosensors intravenously (i.v.). This approach, however, is limited to diseases that are active at the time of administration, due to the rapid depletion of diagnostic peptides in the bloodstream. Instead, we chose to exploit recently developed insights into trafficking of nanoparticles delivered to the subcutaneous (s.c.) space to develop a sustained-release formulation of synthetic biomarkers.[13] Subcutaneously delivered sustained-release formulations have been developed for delivery of small molecule drugs,[14,15] as well as proteins,[16–18] and have achieved delayed release kinetics over hours to months.[19–22]

In this paper, we present a sustained-release synthetic biomarker system designed to be administered at the time of hospital discharge and repeatedly measured using a paper point-of-care (POC) assay. We formulated an exogenous nanosensor that was optimized for delivery under the skin (subcutaneously) and subsequent diffusion into the bloodstream, in contrast to nanomaterials aimed at improving lymph node accumulation.[13] We demonstrate that nanoparticles of small enough size are able to enter the bloodstream efficiently, while still avoiding urinary excretion. We first evaluated the pharmacokinetic (PK) properties of these nanosensors in mice and implemented a PK model to identify guidelines for their application. We constructed two different sets of synthetic biomarkers, demonstrated their responsiveness to disease-associated proteases in vitro, and evaluated their utility in either diagnosing PE or measuring inflammation associated with pneumonia using urinary readouts to enable ease of sample and data collection. Finally, we developed a vertical flow assay paper ELISA (Enzyme-linked immunosorbent assay) test that offers several desirable attributes over typical paper strip tests (LFAs). Paper ELISAs are easy to assemble, have quantitative readouts and small footprints, and avoid false negatives at high sample concentrations, as is common with LFA tests.[23,24]

2. Results and Discussion

2.1. Design of Subcutaneously Delivered Synthetic Biomarkers

We selected an updated design structure of the scaffold holding the protease-sensitive reporters. Specifically, in place of iron oxide particles that have been employed in most of our existing synthetic biomarkers, we utilized a large poly(ethylene glycol) (PEG) 40 kDa scaffold as a chaperone for urinary biomarkers as it is inexpensive, has minimal uptake by the RES (reticuloendothelial system), and exhibits "stealth" behavior.[25–27] Additionally, cellular uptake of particles by numerous cell types, including macrophages, has been minimized with PEG coatings,[28,29] which makes this scaffold ideally suited for subcutaneous injections. Peptide sequences designed for their selective protease sensitivity were linked to urinary reporters (collectively referred to as synthetic biomarkers) and coupled to multiarm PEG (eight reactive groups) scaffold molecules (**Figure 1**).

In addition to selecting the nanoparticle chaperone core, we further designed the reporter component of our subcutaneous synthetic biomarkers to comprise a protease-resistant D-stereoisomer of glutamate-fibrinopeptide B and contain either fluorescein (FAM) or dinitrophenyl (DNP) and a biotin for ELISA detection (Figure S1a,b of Supporting Information).[10,11] Synthetic peptide substrates can be chosen to be efficiently cleaved by disease-associated proteases of interest, thereby releasing urinary reporters (Figure 1a). Combined, these PEG-chaperoned synthetic biomarkers have been designed to be dosed into the subcutaneous space in a large bolus that will enable transport into the bloodstream over an extended period of time. After circulation-mediated transport of the synthetic biomarkers to the site of disease and subsequent proteolysis, liberated reporters are concentrated in the kidney and clear the body via the urine, allowing for quantification using either conventional ELISA[10] or paper ELISA (Figure 1b).

The hydrodynamic diameter of the 40 kDa PEG scaffolds in PBS was measured by dynamic light scattering and found to be approximately 8 nm (**Figure 2**a, Figure S2 of Supporting Information). This size falls in an ideal range for the subcutaneous delivery of synthetic biomarkers to the bloodstream, as smaller particles (<5 nm) are efficiently cleared through the kidneys even in the absence of protease-mediated cleavage,[30,31] which would confound urine measurements, and larger particles (>10 nm) will primarily drain to the lymphatic vessels.[13,32,33] Recently, we characterized the urinary clearance of various sizes of PEG scaffolds after an i.v. injection, and validated that 40 kDa PEG is not renally filtered into urine.[34]

2.2. PEG Synthetic Biomarkers Are Selectively Responsive to Proteases

We first sought to confirm whether peptides coupled to PEG molecules could still be cleaved by proteases, as the presentation of substrates on surfaces can alter the kinetics of cleavage.[35] A fluorogenic version of the thrombin-sensitive peptide (Name: T1Q, Table S1 of Supporting Information) was conjugated to the PEG scaffold to enable detection of cleavage by monitoring for an increase in fluorescent signal. As predicted, recombinant thrombin cleaved the PEG-conjugated peptide, whereas this substrate was poorly cleaved by an alternative clotting cascade protease, factor IX (Figure 2b). Additionally, we tested the responsiveness of our sensors to clotting signals in serum by adding $CaCl_2$ to normal serum to induce clotting. Consistent with the findings observed using recombinant proteases, initiation of the clotting process was followed by a dramatic increase in fluorescence, yet the signal in serum was unchanged with the addition of PBS. The addition of the direct thrombin inhibitor, Argatroban, eliminated the fluorescence increase observed in response to $CaCl_2$, supporting the interpretation that the observed signal was thrombin-mediated (Figure 2c).

We performed a parallel characterization using a substrate selected for its responsiveness to MMP9, based on observed enhanced activity of this enzyme during the inflammatory response to infection.[5,36–38] We developed a fluorogenic version

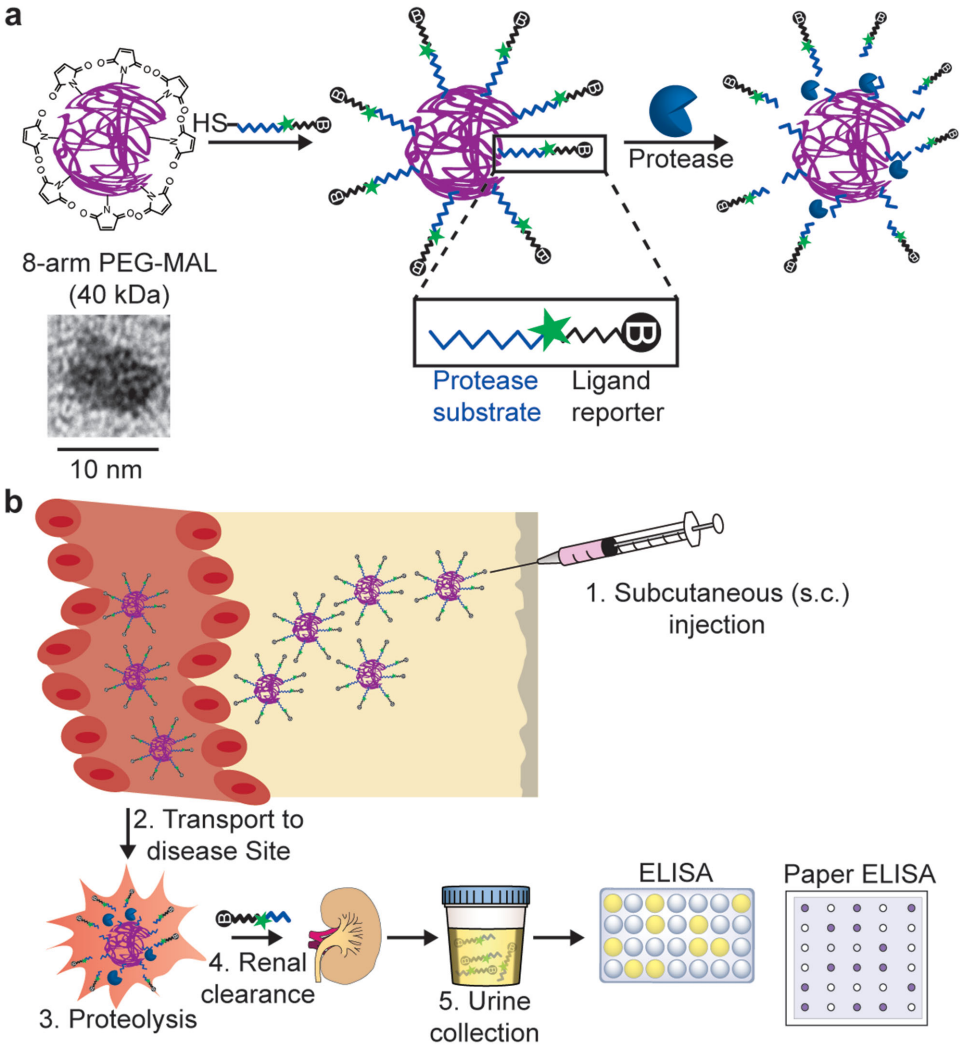

Figure 1. Design of subcutaneously administered synthetic biomarkers. a) Eight-arm PEG-maleimide (PEG-MAL) was reacted with cysteine-terminated peptides comprising of urinary reporters and protease substrates. Proteolysis of the substrates releases reporters that clear into the urine. Image is a transmission electron micrograph of the PEG molecules. b) These PEG-chaperoned synthetic biomarkers are small enough to enter the bloodstream over an extended period of time after a subcutaneous injection. They can survey the host vasculature and respond to disease-associated proteolysis. After urinary clearance of cleaved reporters, a conventional ELISA or paper ELISA can be used for analysis.

(Name: M1Q, Table S1 of Supporting Information) of this peptide and incorporated it on the PEG scaffold. When MMP9 was added to the PEG peptides, we observed that the proteolysis of the substrates was abrogated in the presence of an MMP inhibitor, Marimastat (Figure 2d). By contrast, a distinct enzyme, MMP19, did not cleave this substrate.

As a final characterization of the PEG-peptide pairing of our biomarker design, we sought to determine the stability of the particles, since their use in long term or serial monitoring will require that they remain intact in the absence of proteases while under physiological conditions. PEG-T1Q was incubated in control serum overnight at 37 °C and then exposed to recombinant thrombin. The resulting fluorescent signal indicated that overnight-incubated particles were equally responsive to cleavage as fresh particles (Figure S3, Supporting Information). Furthermore, particles that were frozen, stored at room temperature, or placed at 37 °C each responded to proteases in a similar manner as particles stored at 4 °C (Figure S4, Supporting Information). This degree of stability should enable flexible transport and storage of these particles for use in POC applications.

2.3. Pharmacokinetic Performance of Subcutaneously Administered PEG Chaperones

We next wanted to confirm our hypothesis that 40 kDa PEG particles are ideally suited for s.c. administration by characterizing their pharmacokinetic properties in vivo. We compared the transport kinetics to the bloodstream from a subcutaneous injection of fluorescently labeled 40 kDa PEG, 20 kDa PEG, and iron oxide nanoparticles (≈30 nm) by collecting serial blood samples after the injection. 40 kDa PEG performed similarly to 20 kDa PEG and significantly better than iron oxide particles.

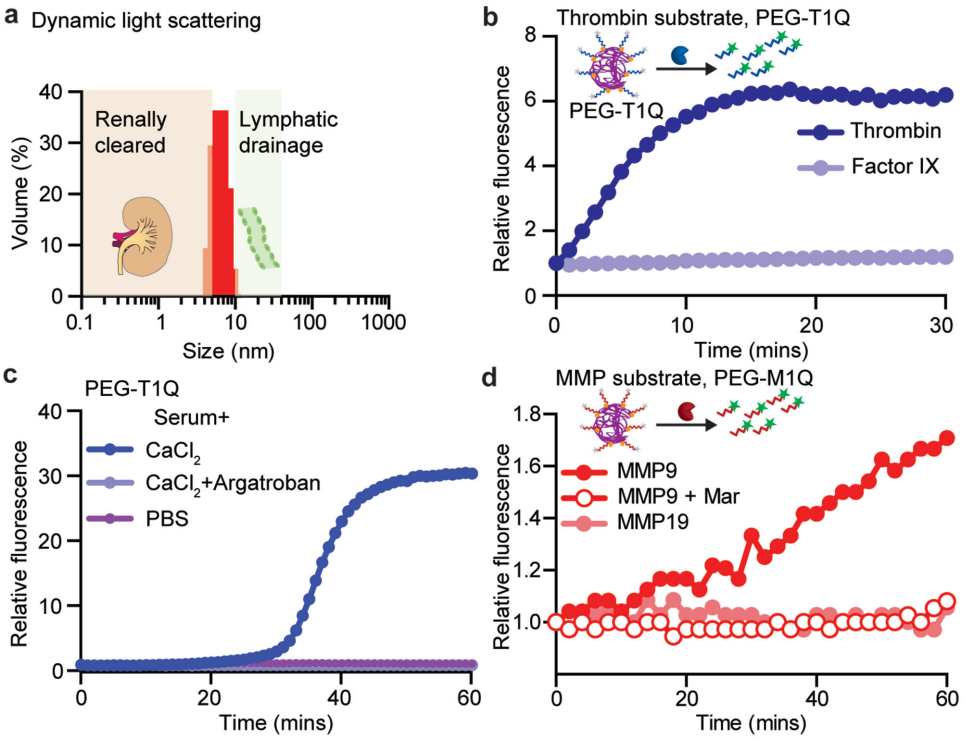

Figure 2. In vitro characterizations of PEG-peptide substrates. a) Dynamic light scattering measurements of PEG backbones. b) PEG-T1Q (thrombin substrate) was exposed to recombinant proteases involved in the clotting cascade. Representative dequenching measurements after protease addition. c) Sensors were responsive to the natural process of clotting by adding $CaCl_2$ to activate clotting in human serum. Addition of the thrombin inhibitor, Argatroban, mitigated the cleavage of the substrates. d) PEG-M1Q (MMP9 substrate) was exposed to MMPs. MMP9 cleavage of the substrate was blocked by the MMP inhibitor Marimastat.

The 20 kDa PEG particles had slightly more rapid permeation to blood but were rapidly depleted, consistent with the hypothesis that smaller particles would have faster kinetics of entry to the bloodstream from a subcutaneous injection but would be renally filtered (**Figure 3**a). We observed that delivery to the blood from the bolus was linear over a period of 8 h. Blood half-life was measured by infusing 40 kDa PEG intravenously and measuring concentration in serial blood samples (Figure 3b). A half-life of greater than 20 h was measured by fitting this data to a one-phase exponential decay model. Therefore, we validated the use of 40 kDa PEG scaffolds for s.c. delivery.

With this data in hand, we sought to dissect the kinetics of permeation into the bloodstream and the persistence of the particles due to backbone half-life. We modified a pharmacokinetic model comprised of a system of ordinary differential equations (ODEs) previously developed in our laboratory and shown to be capable of predicting synthetic biomarker kinetics in vivo.[34] We fit the gathered data for 40 kDa PEG to a model that accounted for nanoparticle entry into the bloodstream followed by clearance with a half-life of 24 h. Two rate constants were fit to the data; the first, expressed as a simple multiplication of a rate constant by the concentration difference between the two compartments, addressed nanoparticle transport from the subcutaneous bolus to blood. The second rate constant addressed the rate of nanoparticle (NP) clearance in the s.c. space (e.g., by macrophages or adsorption). The fitted rate constant ($k_{PEG40k,\ blood}$) and rate constant of clearance ($k_{clear,\ sc}$) were found to be 1.88×10^{-4} min^{-1} and 7.48×10^{-4} min^{-1}, respectively (Figure S5 of Supporting Information; Table S2 of Supporting Information). Here, we quantified the pharmacokinetics of the PEG scaffold, which is expected to be significantly more persistent in blood than the peptide due to rapid proteolysis and subsequent renal clearance.

We next measured the dynamics of background urine reporter signal generation in healthy mice from a subcutaneous administration of PEG-chaperoned synthetic biomarkers. We delivered PEG-T1E (Name: T1E, Table S1 of Supporting Information), which bore the thrombin-sensitive substrate and urinary reporter, subcutaneously and collected urine over a 24-h time period. Urinary reporter concentration associated with background protease levels in the healthy mice was quantified using an ELISA for the FAM/biotin components of the reporters (Figure S1a, Supporting Information). We observed an increase in urine signal for approximately 3 h after administration, and a quantifiable urine signal was maintained for an extended period of time (Figure 3c). This observation supports our proposal to use s.c. compatible synthetic biomarkers for extended periods of time to enable disease detection during the period in which protease substrates are being added to the circulation from the subcutaneous injection site.

To gain a more quantitative understanding of the time scales for the use of s.c. administered synthetic biomarkers, we extended our model to account for proteolysis of peptide substrates in vivo. We used parameters established by our group for catalytic efficiency of proteases for our chosen substrates and the concentration of active, corresponding proteases in

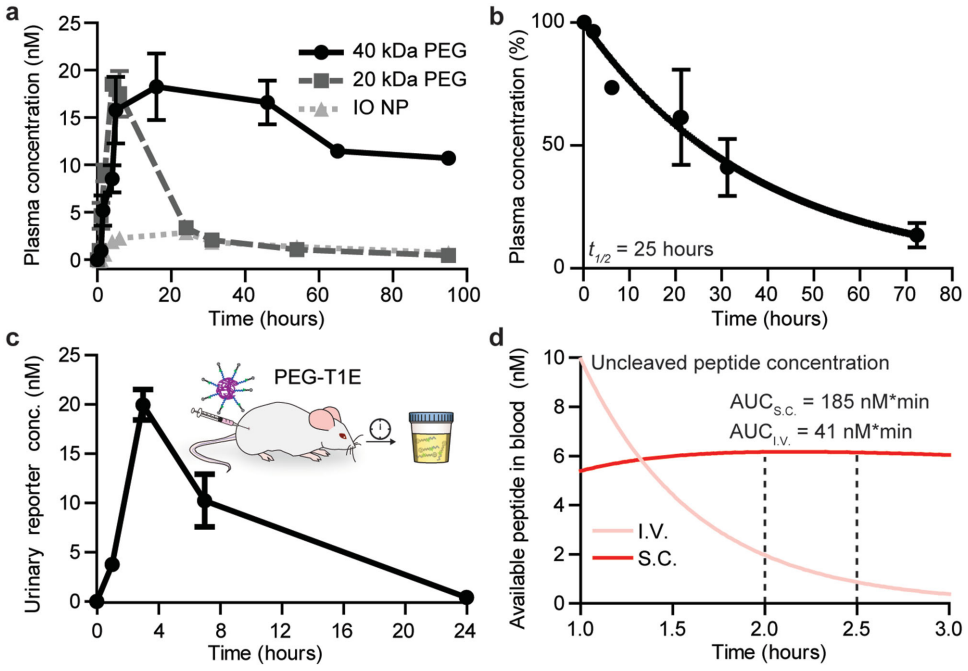

Figure 3. In vivo pharmacokinetics of PEG-chaperoned synthetic biomarkers. a) Kinetics of transport to the bloodstream after a subcutaneous injection of fluorescently labeled PEG or iron oxide nanoparticle (IO NP) backbones. Injected dose (I.D.) = 1000 pmoles for all particles. b) Blood half-life of fluorescently labeled PEG backbones (I.D. = 200 pmoles). Blood half-life was calculated by fitting the data to a one-phase exponential decay. c) PEG-T1E (I.D. = 1000 pmoles) was injected s.c. into healthy mice and urine was collected for 24 h to understand the kinetics of transport, proteolysis, and renal filtration. (a–c: n = 3–4 mice per condition, error bars: ± SEM). d) An ODE model that included all rate constants of transport, clearance, and proteolysis was built and queried for the amount of available peptides in blood after an intravenous or subcutanoues injection. Significantly greater amounts of peptide were modeled to be available after a subcutaneous injection at later time points.

blood (Table S2 of Supporting Information).[34] With this model, we compared the number of available (uncleaved) peptides in blood as a function of time after an i.v. or s.c. injection, with the same initial dose. After approximately 1 h, the amount of uncleaved peptide in circulation from a s.c. injection was predicted to surpass the i.v. injection (Figure 3d). This relationship likely comes about due to the known, rapid depletion of peptide concentration from the bloodstream, in contrast to the case of s.c. delivery, in which peptides are diffusing from the injected bolus to enter circulation. To extend the available number of substrates or modulate the kinetics of the system, it would be possible to increase the concentration of the bolus delivered (Figure S5b,c of Supporting Information), or utilize controlled-release polymers.[21,39]

2.4. In Vivo Thrombosis Diagnosis Enabled by Subcutaneous Administration

After establishing the pharmacokinetic performance of subcutaneously delivered synthetic biomarkers, we tested their ability to diagnose delayed onset disease. We first validated that the PEG synthetic biomarkers could be used to detect ongoing thrombosis in a mouse model that consists of an intravenous injection of thromboplastin, which results in the formation of blood clots, primarily in the lung vasculature, via the extrinsic clotting cascade.[10,40] We further supported the use of this model for our purposes by administering fluorescent fibrinogen in concert with escalating doses of thromboplastin, after which we observed increasing levels of fibrin deposition in the lung (Figure S6, Supporting Information). We extended these experiments by employing the thrombin synthetic biomarker (PEG-T1E) platform to detect pulmonary emboli following their systemic, intravenous administration. Consistent with our work with iron oxide particles,[10] when PEG-chaperoned synthetic biomarkers were coadministered with thromboplastin, urinary signal was significantly elevated when compared to healthy controls, as measured by an ELISA for the encoded reporters (**Figure 4**a). This paradigm, however, does not reflect the kinetics of a clinical scenario in which the onset of a postoperative complication is more likely to be delayed relative to the time of diagnostic administration. When the diagnostic particles were administered intravenously 2 h prior to disease onset, they lacked the capability to distinguish between diseased and healthy animals due to the rapid depletion of protease substrates (Figure 4b). To extend the window of time in which administered synthetic biomarkers have the capacity to read out a response to thromboplastin, we repeated the offset delivery protocol and replaced the i.v. injection with s.c. administration of PEG-T1E. Consistent with our design criteria, and in contrast to the lack of diagnostic power of i.v. delivered synthetic biomarkers, the same dose of s.c. particles administered 2 h prior to disease onset was able to clearly distinguish between diseased and healthy animals (Figure 4b,c). We anticipate that the success of the latter protocol in detecting the PE is based on the remaining bolus of uncleaved peptide

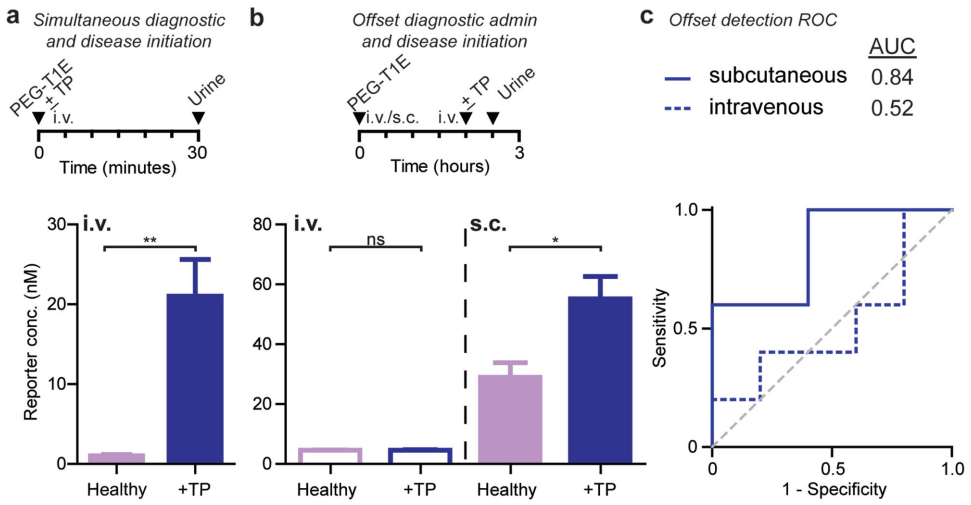

Figure 4. Subcutaneous delivery of synthetic biomarkers enables detection of delayed pulmonary emboli. a) PEG-T1E was able to distinguish between healthy and thrombotic mice when disease onset and diagnostic administration occurred simultaneously. b) In contrast, when the diagnostic was administered intravenously prior to disease onset, synthetic biomarkers were unable to distinguish between diseased and healthy mice. PEG-T1E synthetic biomarkers injected in advance subcutaneously were able to distinguish diseased and healthy mice, as the available concentration of peptides is greater than in the i.v. case. c) Receiver operating characteristic curve shows improved performance of subcutaneously administered particles (a–c: $n = 5$ per condition; ± SEM; one-tailed Mann–Whitney test, $^*P<0.05$, $^{**}P<0.01$).

substrates that can enter the bloodstream throughout the experimental period. The concentrations of nanoparticles used in these experiments are known to be well tolerated in mice and reflect a dose of approximately 5 mg kg^{-1}, which should be well tolerated in humans.[9,34] In the future, determination of ideal concentration for human translation will be necessary. Encouragingly, however, our previous data have suggested that these synthetic biomarkers have steady signal-to-noise ratios across several logs of concentrations.[34,41] Additionally, we have previously developed an orthogonally encoded, free urinary reporter that is coinjected with synthetic biomarkers for use in normalizing hydration state and urinary volume of mice.[10] This normalization capacity will be valuable in accounting for physiologic variability between patients and in dosages delivered in a future clinical setting. Furthermore, as we move to humans, we expect that further studies will be necessary to identify sources of variability in transport in different tissue beds as well as within patient populations.

2.5. Subcutaneously Delivered Synthetic Biomarkers Track Inflammatory Response to Infection

As a second application, we tested the MMP-responsive synthetic biomarker (Name: M1E, Table S1 of Supporting Information) for its ability to detect inflammation associated with pneumonia, as MMPs are released by responding neutrophils and other immune cells as key mediators in innate immunity and inflammation.[36,42] While MMP9 is implicated in several pathologies, such as cancer and fibrosis, we chose it as a broadly important protease relevant to infection. In future evolutions of this platform, improved specificity for a specific bacterial strain could be achieved by designing a synthetic biomarker that responds to known bacterial proteases, such as elastase and LasA from *Pseudomonas aeruginosa*, or SpeB from *Streptococcus pyogenes*. We administered MMP9-sensitive synthetic biomarkers intravenously approximately 24 h after intratracheal inoculation of *P. aeruginosa*, which models one of the most significant postsurgical risks, known as hospital-acquired pneumonia (**Figure 5**a). One hour after i.v. administration of synthetic biomarkers, urine reporter levels measured by ELISA for the DNP/biotin encoded reporters were significantly higher in infected mice compared to healthy controls (Figure 5b). Pulmonary infection was confirmed by quantifying the number of colony forming units (CFUs) of bacteria present in lung homogenates (Figure S7 of Supporting Information). Another key feature of our platform is that the MMP-sensitive

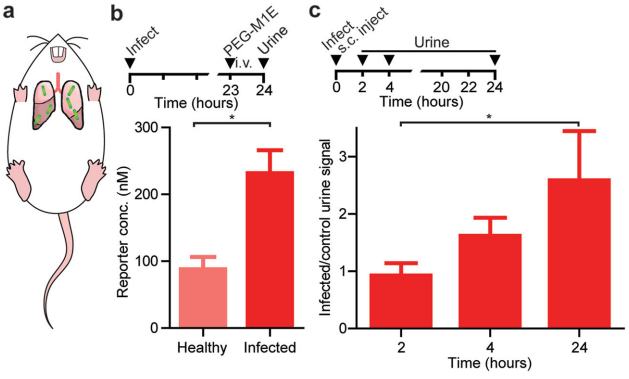

Figure 5. Temporal measurement of inflammatory response to *Pseudomonas aeruginosa* pneumonia. a) Infection was established in mice by intratracheal delivery of *P. aeruginosa* directly to the lung. b) Intravenously delivered PEG-M1E synthetic biomarkers are sensitive to infection 24 h postinfection (I.D. = 400 pmoles). c) Subcutaneously delivered PEG-M1E synthetic biomarkers are able to track the response to infection (I.D. = 4000 pmoles). Two hours postinfection, there is no difference between urine signals from healthy and infected mice, but as the infection progresses, urine signal from infected mice is significantly elevated (b–c: $n = 4$–5 per condition; ± SEM; one-tailed Mann–Whitney test).

reporter sequence was selected to be orthogonally encoded relative to the thrombin reporter, which will enable future multiplexing (Figure S1a of Supporting Information).

After confirming that the M1E synthetic biomarkers have the capacity to detect ongoing pulmonary infections, we tested the ability of subcutaneously delivered particles to detect an infection that developed subsequent to the administration. In other words, we sought to track the immune response after a single administration of nanoparticles as a function of time, which would not be possible using intravenous measures, due to rapid depletion of protease substrates in the bloodstream. A bolus of PEG-M1E particles was administered subcutaneously to cohorts of mice that were either coinfected or not infected via pulmonary delivery of bacteria. Reporter concentration in urine was measured periodically in both groups by ELISA over a 24 h period. Initially, no difference between healthy and infected mice was observed (2 h), but at later time points (24 h) as the inflammatory response strengthened, the urine signal in infected mice was significantly elevated (Figure 5c). The ability to make noninvasive, longitudinal measurements in at-risk individuals should enable the study of additional dynamic processes beyond inflammation and offer the opportunity to detect diseases with varying onset kinetics. For example, a panel of subcutaneously delivered synthetic biomarkers could be administered and followed in order to identify evolving disease signatures in various settings. This insight would be valuable, as proteolytic responses throughout the course of various diseases are dynamic, such as invasion associated with cancer,[43] tissue damage from fibrosis,[44] and infectious diseases.[45] Currently, however, our sensitivity for low burden disease needs improvement, as our proof-of-principle disease models recapitulate high burden disease. Sensitivity can be improved significantly by developing selective substrates that respond more potently to the specific proteases of interest.[34]

2.6. Development of a Companion Paper ELISA

We developed a companion paper test for use in detection of these urinary synthetic biomarkers. Paper tests enable inexpensive and facile diagnosis, which is highly desirable for POC monitoring as the results can be analyzed by direct visualization[46] or by simple, quantitative imaging via cell phones or desktop scanners.[47] We chose to design a paper ELISA to leverage the fact that this combination offers the same benefits of conventional paper tests (e.g., faster and cheaper than conventional assays) and also yields the higher sensitivity of quantitative ELISAs.[23] An additional benefit of a vertical-flow approach, as opposed to typical lateral-flow readouts, is the avoidance of hook effects, where high concentrations result in false negatives.[24] We created paper tests by reflowing wax deposited from a commercial solid ink printer to create an array of test spots on a single piece of paper (**Figure 6**a). During reflowing on a hot plate, printed wax permeates through the paper to create test spots surrounded by hydrophobic barriers (Figure 6b), which can be used as individual reaction wells (Figure 6c). The assay was performed by first drying the detection antibody on test spots, followed by blocking and washing steps. Urine was next added to the test zones, followed by addition of streptavidin alkaline phosphatase (ALP) conjugate as the detection antibody. Bound ALP was exposed to BCIP/NBT (5-bromo-4-chloro-3′-indolyphosphate p-toluidine salt/nitro-blue tetrazolium chloride), which resulted in a purple colored precipitate (Figure 6d).

This sandwich paper ELISA could detect reporters across a wide range of concentrations, with a robust linear response from approximately 1–50 $\times 10^{-9}$ M for the FAM/biotin reporters (Figure 6e). These paper tests were also stable over extended periods of time, enabling storage and transport of the paper test necessary for POC applications (Figure S8 of Supporting Information). We also developed an orthogonal paper test for the DNP/biotin reporter (Figure S9 of Supporting Information), which was not cross-reactive across paper ELISA formats (Figure S10 of Supporting Information).

We tested the ability of these companion paper ELISAs to analyze urine samples to diagnose thrombosis, as described above. Paper analysis of the urine samples yielded the same results as conventional ELISA analysis (Figure 6f,g). We further confirmed that paper DNP ELISAs could be performed on urine from infected mice (Figure S11a of Supporting Information). Signals derived from conventional and paper ELISA tests were significantly positively correlated (Figure S11b of Supporting Information). Additionally, paper ELISA detected an elevated reporter signal in urine sampled at 24 h from infected mice that had received subcutaneous injections compared to healthy mice (Figure S11c of Supporting Information). To accommodate future automation of the detection process, the design of the system is such that all reagents can be preloaded onto the paper tests to enable single step analysis. We envision that this will involve laminating or casing arrays of paper reaction tests. Each reaction test spot would contain preloaded reagents, which could release after addition of urine. With this adaptation of the paper ELISA, we envision that patients may one day apply their own urine sample to a prefabricated test via a dropper, record the result with a smartphone photograph using alignment markers, and electronically submit the outcome to their healthcare team for interpretation. Collectively, our updated synthetic biomarkers are suitable for subcutaneous delivery, and when coupled with paper test analysis, have the capacity to enable simple, sensitive point-of-care monitoring of at-risk patients in order to more effectively detect life-threatening complications in time to prescribe clinical interventions.

3. Conclusions

Here, we developed PEG-chaperoned synthetic biomarkers for subcutaneous delivery to detect blood clots and inflammation associated with pneumonia, two common posthospitalization complications. We characterized the pharmacokinetics of s.c. administered particles and built a mathematical model of their in vivo characteristics. Subcutaneous delivery of synthetic biomarkers allowed for the extended availability of diagnostic peptides, enabling the detection of clots long after diagnostic administration. We additionally applied this system for pneumonia detection over a 24-hour time period. Finally, we developed a companion paper test for the urinary reporters

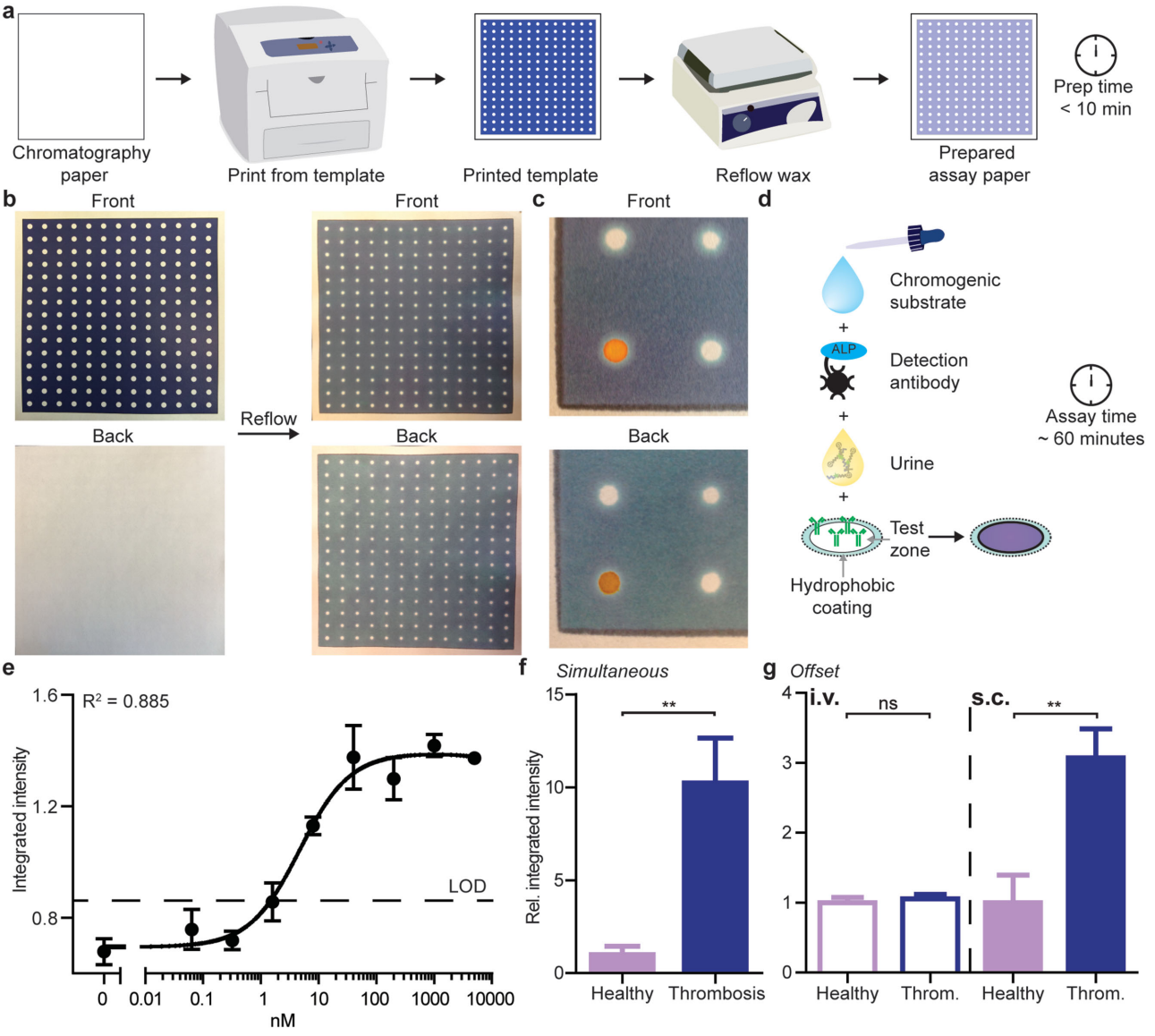

Figure 6. Development of companion paper ELISA for subcutaneously delivered synthetic biomarkers. a) Work flow for creating paper-based assay templates. Paper ELISA spots were printed using a solid ink printer to provide reaction spots surrounded by hydrophobic barriers on chromatography paper (200 × 200 mm). b) Photographs of paper after printing and reflowing. c) Dye added to a reaction spot remains within the spot and travels vertically through the paper. d) Similar to conventional sandwich ELISAs, a primary antibody is used to capture the reporter. Streptavidin-ALP was used as the secondary antibody and exposed to a chromogenic substrate. e) FAM paper ELISA was sensitive to reporter concentration across two logs of concentration, with a strong linear response from approximately 1 to 50 × 10^{-9} M for the FAM/biotin reporters ($n = 3$, error bars: ± SEM, curve fit: one site binding fit). f,g) Companion paper ELISAs for urine analysis of the thrombosis diagnosis. Paper analysis of the urine yielded the same results as conventional ELISA readout (see Figure 4).

to enable POC monitoring. Beyond enabling delayed disease diagnosis, subcutaneous delivery of synthetic biomarkers can enable improved adoption and decreased invasiveness of this platform by accommodating commercially available needle-free injection technologies, as these are preferred by patients.[48,49] The application of these approaches in combination with established techniques, such as polymeric release depots or implants,[21,50] with which our synthetic biomarkers are compatible (Figure 12a–c of Supporting Information), may enable long-term monitoring of patients with facile urinary readouts.

4. Experimental Section

Synthesis of Peptides and Peptide-PEG Conjugations: Peptides were either synthesized by CPC Scientific, Inc or Tufts Peptide Core. For recombinant enzyme studies, intramolecularly quenched peptides were used (Table S1 of Supporting Information). In vivo protease-sensitive substrates were synthesized to contain a urinary reporter (a stable D-stereoisomer of glutamate-fibrinopeptide B with a ligand handles) for detection.

Multivalent PEG (40 kDa, eight-arm) containing maleimide reactive handles (JenKem Technology) was dissolved in PBS. Dissolved particles were filtered (pore size: 0.2 µm). After filtration, the cysteine-terminated peptides were added at 20-fold excess to the PEG and reacted for at

least 1 h. Unconjugated peptide was filtered using fast-protein liquid chromatography (FPLC, GE Healthcare) or by spin filters (MWCO = 10 kDa, Millipore). Size measurements were made by dynamic light scattering in PBS (Malvern Instruments Nano ZS90). Transmission electron microscopy was performed at Keck Microscopy Facility at the Whitehead Institute with 2% uranyl acetate on an FEI Tecnai Spirit.

In Vitro Cleavage Assays: PEG-T1Q (1×10^{-6} M by peptide) was mixed with recombinant human thrombin (≈10×10^{-9} M working concentration; Haematologic Technologies) in a 384-well plate at 37 °C in PBS BSA (1% wt/vol). Similar conditions were used for factor IX. Fluorescence was monitored using a microplate reader (either SpectroMax Gemini EM or Tecan Infinite). For plasma studies, PEG-T1Q was mixed with 50 µL of control human plasma (Thermo Scientific) and 50 µL of 80×10^{-3} M $CaCl_2$ (Sigma) to initiate the clotting cascade with or without the thrombin inhibitor (Argatroban Monohydrate, Sigma) or PBS. For serum stability, PEG-T1Q was added to control human serum and placed at 37 °C overnight and then tested for responsiveness to thrombin compared to fresh PEG-T1Q.

PEG-M1Q (1×10^{-6} M by peptide) was mixed with recombinant human MMP9 or MMP19 (≈100×10^{-9} M working concentration, Enzo Life Sciences) in activity buffer (50×10^{-3} M Tris, 150×10^{-3} M NaCl, 5×10^{-3} M $CaCl_2$, 1×10^{-6} M $ZnCl_2$) containing 1% BSA and fluorescence dequenching was monitored. Marimastat (Tocris Bioscience) was added at a final concentration of 5×10^{-6} M. A similar approach was used for storage stability experiments.

In Vivo Pharmacokinetic Measurements: Multiarm PEG (40 or 20 kDa) was reacted with VivoTag-680 (VT680, Perkin Elmer) and purified. Iron oxide particles were synthesized as described previously[9] and also fluorescently labeled. Injections were performed at either 200 pmoles (for intravenous administration) or 1000 pmoles (for subcutaneous administration). Blood was collected by retroorbital draws using microhematocrit tubes (VWR, ≈10 µL) and then immediately transferred into 90 µL of PBS with 5×10^{-3} M EDTA and spun at 1000×g to pellet blood cells. Concentration was measured using an Odyssey Infrared scanner (Li-Cor Inc.). For urine signal dynamics, 1000 pmoles PEG-T1E was injected s.c. and urine was collected subsequently over a 24-hour time period. Urine was collected by placing mice in custom-devised sleeves with a 96-well plate base. Urine signal was measured using a sandwich ELISA for the fluorescein or DNP and biotin ligand handles as described preivously.[10] Briefly, anti-FITC (GeneTex) or anti-DNP (Life Technologies) antibodies were used as the capture antibody and NeutrAvidin-HRP (Horseradish Peroxidase, Pierce) was used as the detection antibody to recognize the N-terminal biotin on the reporter in high-binding plastic well plates. Bound HRP was exposed to Ultra-TMB (Pierce) substrate and the reaction was allowed to progress. The reaction was quenched using 1 M HCl and absorbance measurements were made at 450 nm. All pharmacokinetic measurement experiments were done using female Swiss-Webster mice (Taconic).

Pharmacokinetic ODE Model: For more complete model derivation, see Kwong et al.[34] Briefly, an ODE model was implemented in MATLAB. To identify transport rate constants from a s.c. injection to the plasma, a simple two-compartment model was implemented and fit to the data using the *nlinfit* command, with parameters associated with the measured blood half-life. To add in the biochemical process of proteolysis, parameters were extracted from Kwong et al. for k_{cat}, K_m, and enzyme concentration. The model was implemented for either a s.c. injection or an i.v. injection. Available peptide concetration was defined as the concentration of uncleaved peptides in blood as determined by the model.

Thrombosis Model Validation and Synthetic Biomarker Detection: Bovine lung thromboplastin (BioPharm Laboratories, 100,000 US activity units) was dissolved in 2 mL of sterile PBS. To validate the thromboplastin model, bovine fibrinogen (Sigma) was reacted with VivoTag750 (VT750; Perkin Elmer) for 1 h and purified by spin filters (100 kDa MWCO). Swiss-webster mice were injected i.v. with labeled fibrinogen and thromboplastin of varying doses. 30 min postinjection, mice were euthanized and lungs were extracted and scanned using the Odyssey Infrared scanner. Fibrin fluorescence intensity was quantified using ImageJ (NIH).

Intravenous simultaneous detection was performed by injecting a mixture containing PEG-T1E (200 pmoles) and thromboplastin (20 U g^{-1}) and collecting urine 30 min after injection. Intravenous offset detection was performed by first injecting PEG-T1E i.v. (1000 pmoles) and returning mice to their cage. 2 h postinjection, mice were re-anesthesized and injected with thromboplastin (20 U g^{-1}) and urine was collected 30 min later. Subcutaneous detection was similar to i.v. offset except the first injection was subcutaneous.

Pneumonia Model Validation and Synthetic Biomarker Detection: Female CD1 mice, 5–7 weeks old, were innoculated intratracheally with 1.25×10^6 CFU of *P. aeruginosa* (strain: PA01) in 50 µL of PBS. Bacteria were cultured overnight in LB broth, and then subcultured and grown to log phase (OD600 ≈0.5) before being pelleted and resuspended in sterile PBS to the requisite concentration. Mice were administered buprenorphine and meloxicam several hours after infection. Lung infection was confirmed by plating serial dilutions of lung homogenates on LB agar. For longitudinal experiments with subcutaneously delivered particles, healthy or infected mice were dosed with particles and urine was collected over a 24-hour period. Each pooled collection time was 1 h.

Paper ELISA Development and Tests: Whatman No. 1 chromatography paper (GE) was used. Test spots were created by coating areas around each spot with hydrophobic barrier using a PAP pen (Dako) or using a Xerox ColorQube 8570 (solid ink printer) and reflowing on a hot plate (for 3 min at 160 °C). Paper test spots were designed in Adobe Illustrator. For quantification, all measurements were performed at least twice.

The assay was performed by first adding the detection antibody (3 µL; GeneTex for antifluorescein, Life Technologies for anti-DNP), followed by a wash using PBS with 1% (w/v) Tween 80. Spots were blocked using PBS with 3% BSA (w/v). After another round of washes, samples or ladder reporters were added, allowed to incubate, and washed. ALP conjugated to streptavidin (Pierce) was added and incubated. Finally, the ALP substrate, BCIP/NBT (Pierce), was added, which upon exposure to ALP forms a purple precipitate. Paper ELISAs were scanned using a desktop scanner and quantified using ImageJ or a custom MATLAB script (see below).

MATLAB Script for Paper ELISA Analysis: All analysis by MATLAB was conducted in the RGB colorspace. First the paper ELISA was imaged using a desktop scanner and saved as a JPEG file. To process the image, MATLAB first thresholded the image in the blue subspace to remove the yellow background. The image was then morphologically opened in order to separate individual wells and remove background pixels that fell outside the threshold range. The regionprops function and thresholding in the red subspace then isolated the red column markers and calculated their respective centroids. The algorithm then identified and labeled connected regions that lay within the x-coordinate of the calculated centroids. The resulting labeled image was then converted to a binary mask and superimposed over the original image to create a labeled image of isolated reaction spots. Finally, the algorithm greenscaled and inverted the image, and then recorded the integrated densities of individual reaction spots.

PLGA Microsphere Release: PEG-VT680 or PEG-T1E was encapsulated in PLGA (Poly(lactic-co-glycolic acid)) 50 lactide:50 glycolide polymeric microspheres using established techniques.[39] Briefly, double emulsion microspheres were formed by adding PEG-T1E in PBS to a PLGA solution in dichloromethane and then adding in polyvinyl alcohol. Solvent was evaporated and microspheres were collected by centrifugation. Release of PEG-VT680 was measured by placing microspheres in PBS at 37 °C and measuring supernatant absorbance. For PEG-T1E, the supernatant was collected and PEG particles were isolated via spin filters (10 kDa MWCO) and exposed to thrombin overnight. Cleaved reporters were isolated via spin filters and measured by ELISA.

Statistics: All statistical analyses were performed in GraphPad (Prism 5.0). Statistical significance and individual tests are described in figure legends.

Animal Protocols: All animal studies were approved by Massachusetts Institute of Technology's Committee on Animal Care.

Supporting Information

Supporting Information is available from the Wiley Online Library or from the author.

Acknowledgements

The authors thank Dr. H. Fleming (MIT) for critical reading and editing of the manuscript, the Koch Institute Swanson Biotechnology Core (MIT), N. Watson (W.M. Keck Microscopy Facility at Whitehead Institute) for TEM, and J. Teixeira (MIT) for access to the solid ink (wax) printer. They thank Andrew Warren (MIT), Dr. Kevin Lin (MIT), Dr. Justin Lo (MIT), and Dr. Ester Kwon (MIT) for helpful discussion. This study was supported in part by a Koch Institute Support Grant P30-CA14051 from the National Cancer Institute (Swanson Biotechnology Center) and a Core Center Grant P30-ES002109 from the National Institute of Environmental Health Sciences. J.S.D. and C.G.B. thank the National Science Foundation Graduate Research Fellowship Program for support. R.T.K.A thanks the UROP office at MIT for funding. G.A.K. holds a Career Award at the Scientific Interface from the Burroughs Wellcome Fund. S.N.B. is a Howard Hughes Institute Investigator.

Received: November 30, 2015
Revised: February 5, 2016
Published online: March 22, 2016

[1] T. Lopes, N. M. Spirtos, R. Naik, J. M. Monaghan, *Bonney's Gynaecological Surgery*, Wiley-Blackwell, Oxford, UK **2010**, p. 52.
[2] A. M. Gillinov, E. A. Davis, A. J. Alberg, M. Rykiel, T. J. Gardner, D. E. Cameron, *Ann. Thorac. Surg.* **1992**, *53*, 988.
[3] N. A. Khan, H. Quan, J. M. Bugar, J. B. Lemaire, R. Brant, W. A. Ghali, *J. Gen. Intern. Med.* **2006**, *21*, 177.
[4] S. Fujitani, H.-Y. Sun, V. L. Yu, J. A. Weingarten, *Chest* **2011**, *139*, 909.
[5] T. S. Wilkinson, A. C. Morris, K. Kefala, C. M. O'Kane, N. R. Moore, N. A. Booth, D. F. McAuley, K. Dhaliwal, T. S. Walsh, C. Haslett, J.-M. Sallenave, A. J. Simpson, *Chest* **2012**, *142*, 1425.
[6] J. S. Ginsberg, P. S. Wells, C. Kearon, D. Anderson, M. Crowther, J. I. Weitz, J. Bormanis, P. Brill-Edwards, A. G. Turpie, B. MacKinnon, M. Gent, J. Hirsh, *Ann. Intern. Med.* **1998**, *129*, 1006.
[7] M. Lorente, M. Falguera, A. Nogues, A. Gonzalez, M. Merino, M. Caballero, *Thorax* **2000**, *55*, 133.
[8] S. Fredericks, S. Guruge, S. Sidani, T. Wan, *Clin. Nurs. Res.* **2010**, *19*, 144.
[9] G. A. Kwong, G. von Maltzahn, G. Murugappan, O. Abudayyeh, S. Mo, I. A. Papayannopoulos, D. Y. Sverdlov, S. B. Liu, A. D. Warren, Y. Popov, D. Schuppan, S. N. Bhatia, *Nat. Biotechnol.* **2013**, *31*, 63.
[10] K. Y. Lin, G. A. Kwong, A. D. Warren, D. K. Wood, S. N. Bhatia, *ACS Nano* **2013**, *7*, 9001.
[11] A. D. Warren, G. A. Kwong, D. K. Wood, K. Y. Lin, S. N. Bhatia, *Proc. Natl. Acad. Sci. USA* **2014**, *111*, 3671.
[12] J. S. Dudani, P. K. Jain, G. A. Kwong, K. R. Stevens, S. N. Bhatia, *ACS Nano* **2015**, *9*, 11708.
[13] L. M. Kaminskas, C. J. H. Porter, *Adv. Drug Deliv. Rev.* **2011**, *63*, 890.
[14] M. Ochoa, C. Mousoulis, B. Ziaie, *Adv. Drug Deliv. Rev.* **2012**, *64*, 1603.
[15] J. W. Lee, J.-H. Park, M. R. Prausnitz, *Biomaterials* **2008**, *29*, 2113.
[16] S. P. Baldwin, W. Mark Saltzman, *Adv. Drug Deliv. Rev.* **1998**, *33*, 71.
[17] Y. Tabata, Y. Ikada, *Adv. Drug Deliv. Rev.* **1998**, *31*, 287.
[18] T. P. Richardson, M. C. Peters, A. B. Ennett, D. J. Mooney, *Nat. Biotechnol.* **2001**, *19*, 1029.
[19] K. E. Uhrich, S. M. Cannizzaro, R. S. Langer, K. M. Shakesheff, *Chem. Rev.* **1999**, *99*, 3181.
[20] J. M. Anderson, M. S. Shive, *Adv. Drug Deliv. Rev.* **2012**, *64*, *Supplement*, 72.
[21] R. S. Langer, N. A. Peppas, *Biomaterials* **1981**, *2*, 201.
[22] S. Mitragotri, P. A. Burke, R. Langer, *Nat. Rev. Drug Discov.* **2014**, *13*, 655.
[23] C.-M. Cheng, A. W. Martinez, J. Gong, C. R. Mace, S. T. Phillips, E. Carrilho, K. A. Mirica, G. M. Whitesides, *Angew. Chem. Int. Ed.* **2010**, *49*, 4771.
[24] B. O'Farrell, *Lateral Flow Immunoassay* (Eds: R. Wong, H. Tse), Humana Press, Totowa, NJ **2009**, 1.
[25] K. Knop, R. Hoogenboom, D. Fischer, U. S. Schubert, *Angew. Chem. Int. Ed.* **2010**, *49*, 6288.
[26] J. M. Harris, R. B. Chess, *Nat. Rev. Drug Discov.* **2003**, *2*, 214.
[27] F. M. Veronese, G. Pasut, *Drug Discov. Today* **2005**, *10*, 1451.
[28] T. J. Harris, G. von Maltzahn, M. E. Lord, J.-H. Park, A. Agrawal, D.-H. Min, M. J. Sailor, S. N. Bhatia, *Small Weinh. Bergstr. Ger.* **2008**, *4*, 1307.
[29] A. S. Zahr, C. A. Davis, M. V. Pishko, *Langmuir* **2006**, *22*, 8178.
[30] H. Soo Choi, W. Liu, P. Misra, E. Tanaka, J. P. Zimmer, B. Itty Ipe, M. G. Bawendi, J. V. Frangioni, *Nat. Biotechnol.* **2007**, *25*, 1165.
[31] M. Longmire, P. L. Choyke, H. Kobayashi, *Nanomed.* **2008**, *3*, 703.
[32] Y. Xie, T. R. Bagby, M. Cohen, M. L. Forrest, *Expert Opin. Drug Deliv.* **2009**, *6*, 785.
[33] F. Zhang, G. Niu, G. Lu, X. Chen, *Mol. Imaging Biol.* **2010**, *13*, 599.
[34] G. A. Kwong, J. S. Dudani, E. Carrodeguas, E. V. Mazumdar, S. M. Zekavat, S. N. Bhatia, *Proc. Natl. Acad. Sci. USA* **2015**, *112*, 12627.
[35] R. Trzcinska, K. Balin, J. Kubacki, M. E. Marzec, R. Pedrys, J. Szade, J. Silberring, A. Dworak, B. Trzebicka, *Langmuir* **2014**, *30*, 5015.
[36] W. C. Parks, C. L. Wilson, Y. S. López-Boado, *Nat. Rev. Immunol.* **2004**, *4*, 617.
[37] B. Schaaf, C. Liebau, V. Kurowski, D. Droemann, K. Dalhoff, *BMC Pulm. Med.* **2008**, *8*, 12.
[38] A. A. El-Solh, D. Amsterdam, A. Alhajhusain, M. E. Akinnusi, R. G. Saliba, S. V. Lynch, J. P. Wiener-Kronish, *J. Infect.* **2009**, *59*, 49.
[39] H. K. Makadia, S. J. Siegel, *Polymers* **2011**, *3*, 1377.
[40] E. J. Weiss, J. R. Hamilton, K. E. Lease, S. R. Coughlin, *Blood* **2002**, *100*, 3240.
[41] A. D. Warren, S. T. Gaylord, K. C. Ngan, M. Dumont Milutinovic, G. A. Kwong, S. N. Bhatia, D. R. Walt, *J. Am. Chem. Soc.* **2014**, *136*, 13709.
[42] T. N. Mayadas, X. Cullere, C. A. Lowell, *Annu. Rev. Pathol. Mech. Dis.* **2014**, *9*, 181.
[43] C. López-Otín, L. M. Matrisian, *Nat. Rev. Cancer* **2007**, *7*, 800.
[44] D. Schuppan, N. H. Afdhal, *Lancet* **2008**, *371*, 838.
[45] P. J. Rosenthal, P. S. Sijwali, A. Singh, B. R. Shenai, *Curr. Pharm. Des.* **2002**, *8*, 1659.
[46] N. R. Pollock, J. P. Rolland, S. Kumar, P. D. Beattie, S. Jain, F. Noubary, V. L. Wong, R. A. Pohlmann, U. S. Ryan, G. M. Whitesides, *Sci. Transl. Med.* **2012**, *4*, 152ra129.
[47] O. Mudanyali, S. Dimitrov, U. Sikora, S. Padmanabhan, I. Navruz, A. Ozcan, *Lab. Chip* **2012**, *12*, 2678.
[48] M. R. Prausnitz, R. Langer, *Nat. Biotechnol.* **2008**, *26*, 1261.
[49] M. R. Prausnitz, S. Mitragotri, R. Langer, *Nat. Rev. Drug Discov.* **2004**, *3*, 115.
[50] R. Langer, *Science* **1990**, *249*, 1527.

ADVANCED FUNCTIONAL MATERIALS

Supporting Information

for *Adv. Funct. Mater.*, DOI: 10.1002/adfm.201505142

Sustained-Release Synthetic Biomarkers for Monitoring Thrombosis and Inflammation Using Point-of-Care Compatible Readouts

*Jaideep S. Dudani, Colin G. Buss, Reid T. K. Akana, Gabriel A. Kwong, and Sangeeta N. Bhatia**

Supplemental Information

Sustained-release synthetic biomarkers for monitoring thrombosis and inflammation using point-of-care compatible readouts

Jaideep S. Dudani[1,2], Colin G. Buss[1,3], Reid T.K. Akana[1,2], Gabriel A. Kwong[1,3,&], and Sangeeta N. Bhatia[1,3-7,]*

1. Koch Institute for Integrative Cancer Research, Massachusetts Institute of Technology, Cambridge, MA 02139
2. Department of Biological Engineering, Massachusetts Institute of Technology, Cambridge, MA 02139
3. Institute for Medical Engineering and Science, Massachusetts Institute of Technology, Cambridge, MA 02139
4. Electrical Engineering and Computer Science, Massachusetts Institute of Technology, Cambridge, MA 02139
5. Department of Medicine, Brigham and Women's Hospital and Harvard Medical School, Boston, MA 02115
6. Broad Institute of Massachusetts Institute of Technology and Harvard, Cambridge, MA 02139
7. Howard Hughes Medical Institute, Cambridge, MA 02139

& Present Address: Wallace H. Coulter Department of Biomedical Engineering, Georgia Tech and Emory School of Medicine, Atlanta, GA 30332

*Corresponding Author:
Sangeeta N. Bhatia
Address: 500 Main Street, 76-453, Cambridge, MA 02142, USA
Phone: 617-253-0893
Fax: 617-324-0740
Email: sbhatia@mit.edu

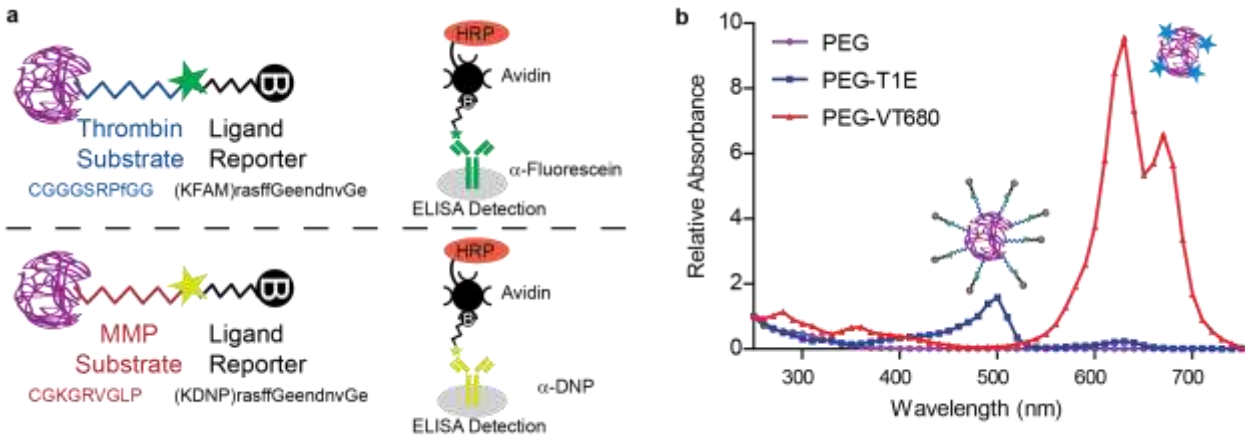

Supplementary Figure 1. Subcutaneously delivered synthetic biomarker particles and design. (**a**) Orthogonally encoded ligand urinary reporters for thrombin and MMP substrates can be detected by custom sandwich ELISAs (**b**) Conjugations of fluorescein-coupled thrombin substrate to multivalent PEG (PEG-T1E) shows characteristic 490 nm peak and conjugation of NHS-VT680 to PEG (PEG-VT680) shows characteristic peaks around 650 nm.

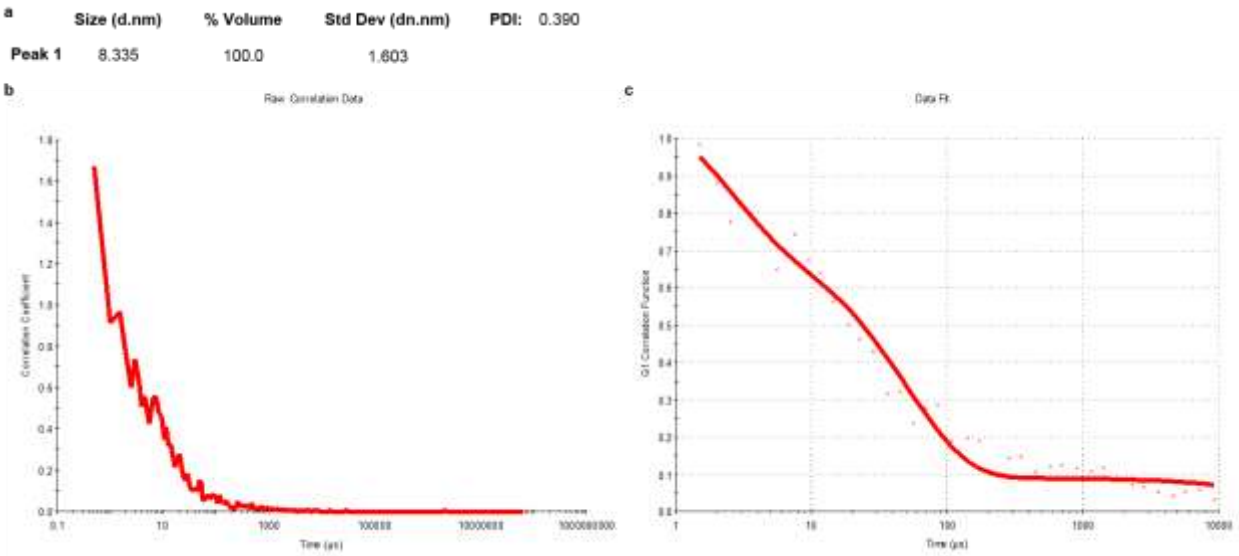

Supplementary Figure 2. Dynamic Light Scattering of PEG scaffolds. (**a**) Peak characteristics of DLS data. (**b**) Raw correlation data and (**c**) data fit from DLS measurement.

Supplementary Table 1. Peptides used throughout study.

Peptide Name	Sequence	Readout	Application
T1Q	5FAM-GGfPRSGGGK(CPQ2)-PEG2-C	Fluorescence dequenching of 5FAM	In vitro thrombin cleavage (Fig. 2b-c)
M1Q	5FAM-GGPLGVRGKK(CPQ2)-PEG2-C	Fluorescence dequenching of 5FAM	In vitro MMP cleavage (Fig. 2d)
T1E	Biotin-eGvndneeGffsar(KFAM)GGfPRSGGGGC	ELISA for FAM and Biotin	Pharmacokinetic characterization and thrombosis detection (Fig. 3c, 4)
M1E	Biotin-eGvndneeGffsar(KDNP)GGPLGVRGKGC	ELISA for DNP and Biotin	Infection response detection (Fig. 5)

Legend

Fluorophore Protease substrate Urinary reporter Coupling to PEG

Quencher Molecular spacers ELISA ligand handles

lower case = D stereoisomer

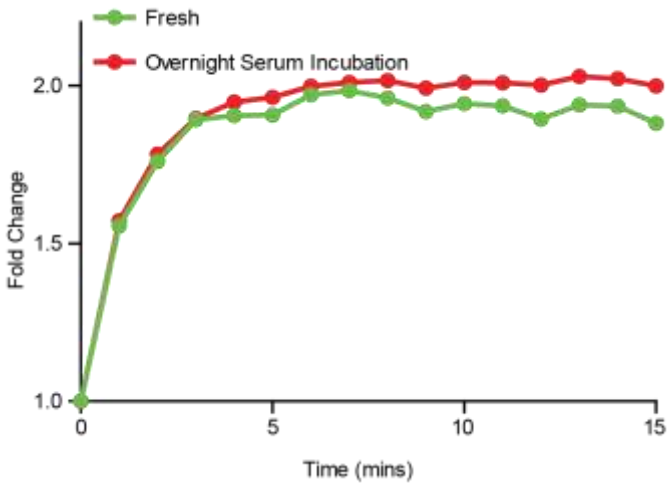

Supplementary Figure 3. Stability in control serum. PEG-T1Q was incubated overnight in human control serum at 37 ºC and then exposed to recombinant thrombin. Fluorescence dequenching was measured and compared to PEG-T1Q that was stored at 4 ºC in PBS.

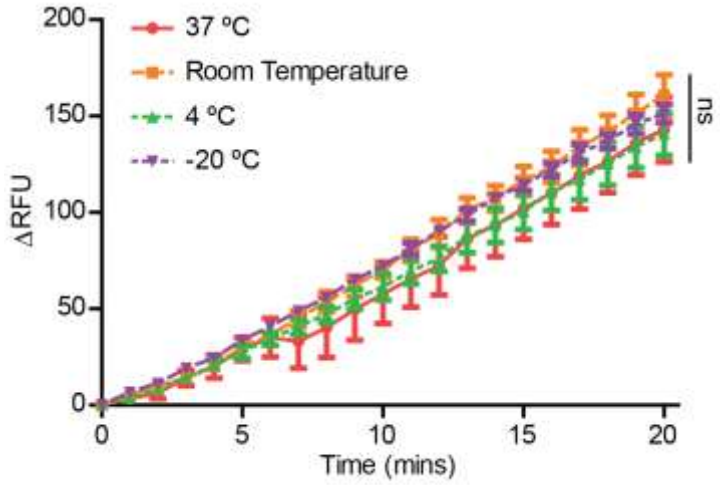

Supplementary Figure 4. Storage stability at varying temperatures. PEG-M1Q was stored at varying temperatures for approximately 24 hours in PBS and then exposed to MMP9. Fluorescence dequenching was measured and compared. PEG-M1Q from all conditions behaved similarly enabling simple particle storage and transport (conditions not significant, P>0.5, by 2way ANOVA).

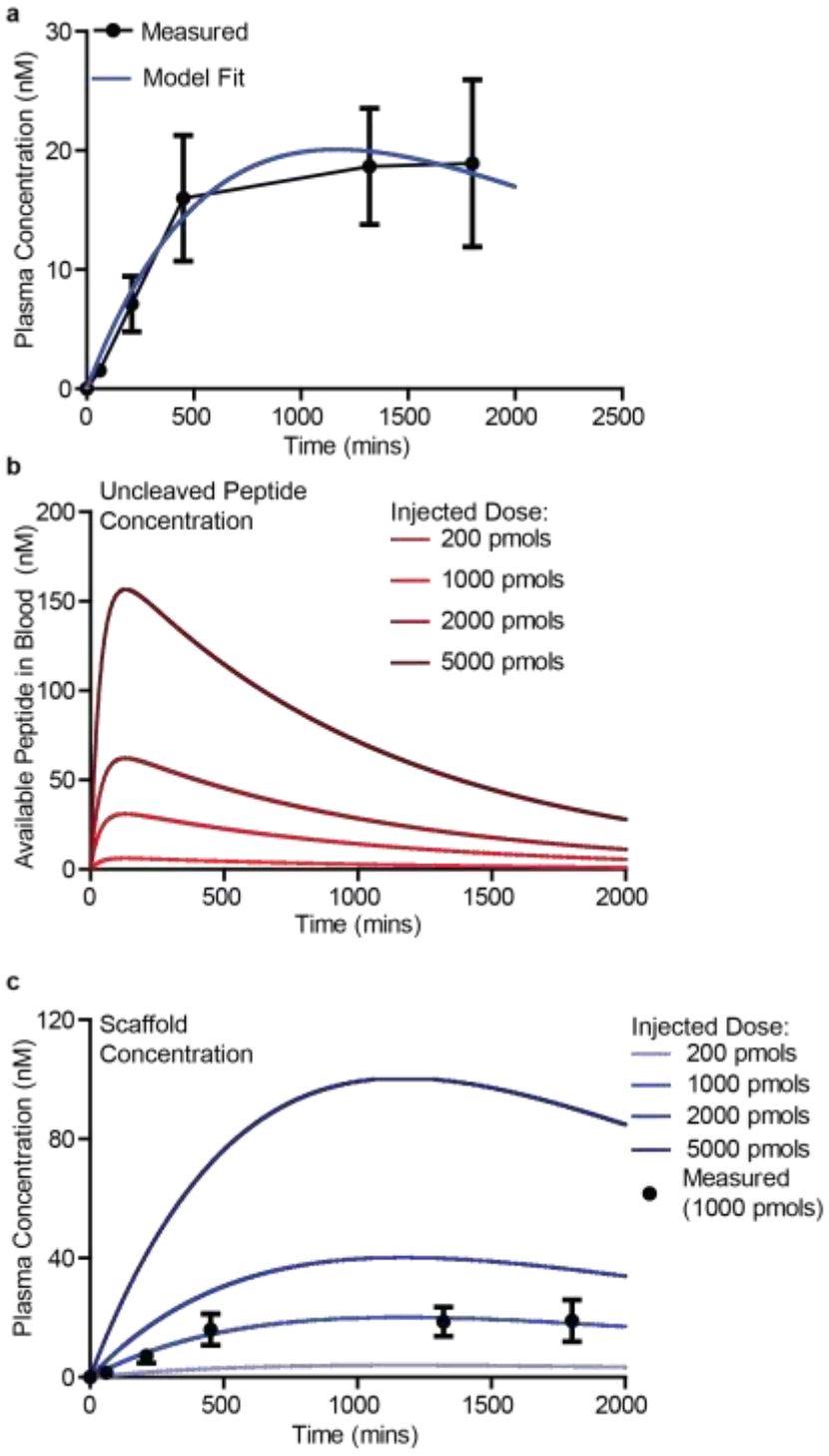

Supplementary Figure 5. Pharmacokinetic model of subcutaneously delivered synthetic biomarkers. (**a**) PEG-VT680 (40 kDa) was injected subcutaneously and blood concentrations were measured. A multi-compartment pharmacokinetic model was built and transport parameters were fit (see next table). (**b**) Uncleaved peptide concentration (e.g. substrate) as a function of time with varying injected doses. (**c**) Scaffold concentration (e.g. PEG backbone) as a function of time with varying injected doses.

Supplementary Table 2. Pharmacokinetic model parameters in mice.

Description	Variable Name	Value	Source
Permeability of NPs from s.c. to blood:	$k_{PEG, blood}$	1.88×10^{-4} min^{-1}	Fit to data
Clearance of NPs in s.c. space:	$k_{clear, sc}$	7.48×10^{-4} min^{-1}	Fit to data
NP clearance via mononuclear phagocyte system	mps_{NP}	5.99×10^{-4} min^{-1}	Based on NP half-life
Catalytic efficiency of proteases in blood	k_{cat}	0.0659 min^{-1}	Kwong et al. (2015)
Michaelis-Menten constant of proteases in blood	K_M	1.00×10^{-5} M	Kwong et al. (2015)
Approximate concentration of blood proteases that cleave substrate	E_b	4.00×10^{-6} M	Kwong et al. (2015)

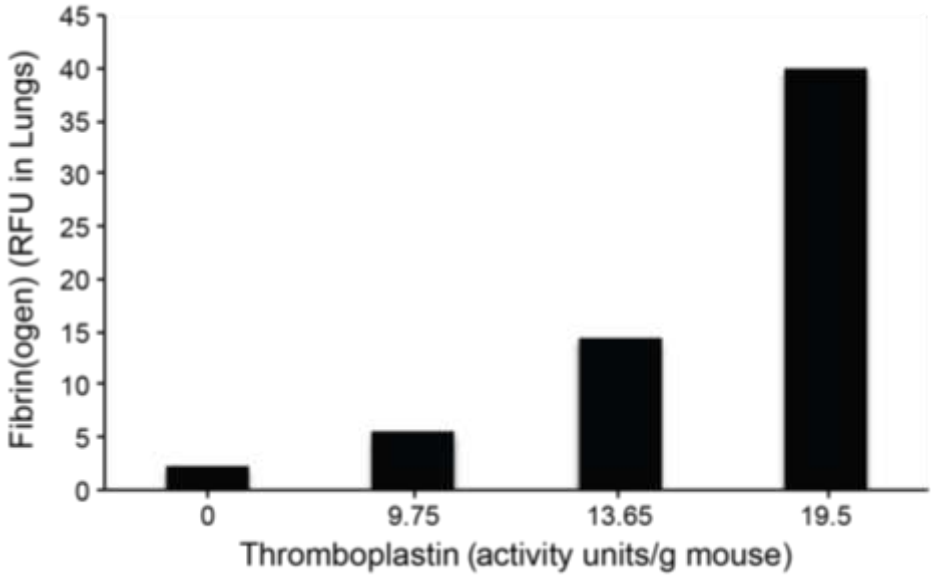

Supplementary Figure 6. Validation of thromboplastin model. Increasing doses of thromboplastin was coinjected with fluorescently labeled fibrinogen. One hour post-injection mice were euthanized and lung fibrin fluorescence was measured. Increasing thromboplastin resulted in greater lung fluorescence demonstrating fibrin deposition by thrombin.

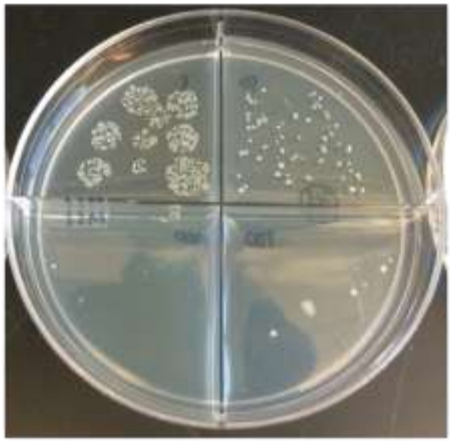

Supplementary Figure 7. Validation of infection. CFU assay to validate infection in lung was performed with dilutions from lung homogenates.

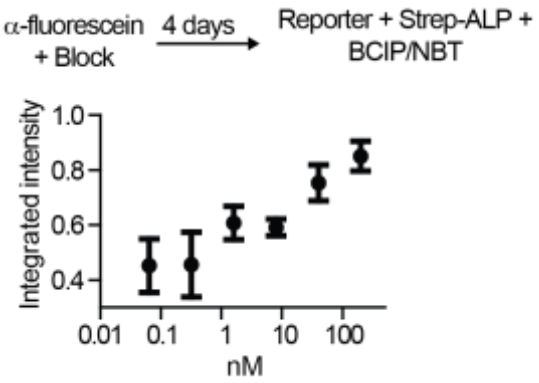

Supplementary Figure 8. Stability of paper ELISA. Anti-fluorescein antibodies and blocking buffer were dried onto paper and stored for four days at 4 ºC. FAM-encoded reporters were added and tested, showing similar behavior to freshly prepared paper ELISAs.

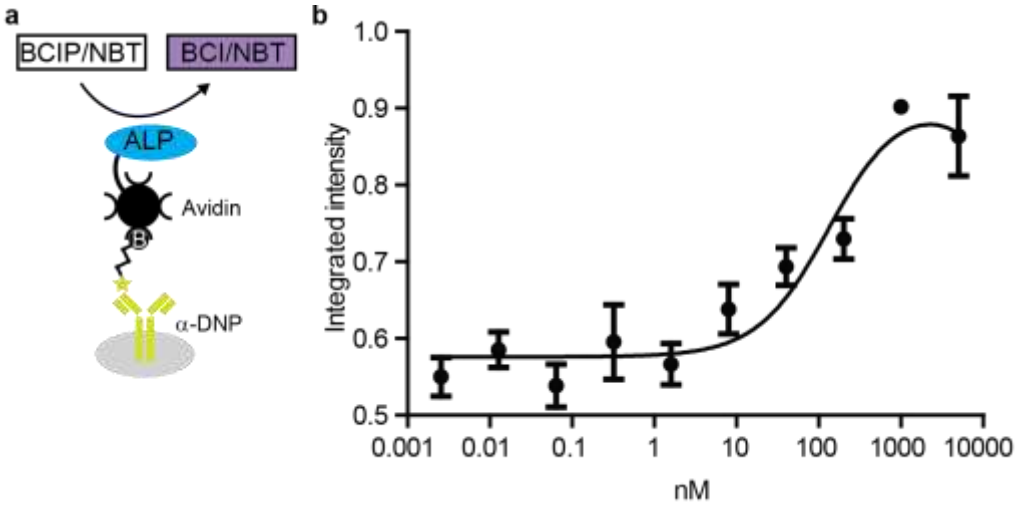

Supplementary Figure 9. Paper ELISA for DNP-encoded reporters. (**a**) Anti-DNP antibodies are dried onto paper test spots and used as the primary antibody. Streptavidin-ALP was used as the secondary. Bound ALP is exposed to BCIP/NBT, which is converted to a purple precipitate. (**b**) Ladder with increasing concentration of DNP reporter shows strong correlation with a binding curve fit with linear region approximately from 1 to 100 nM.

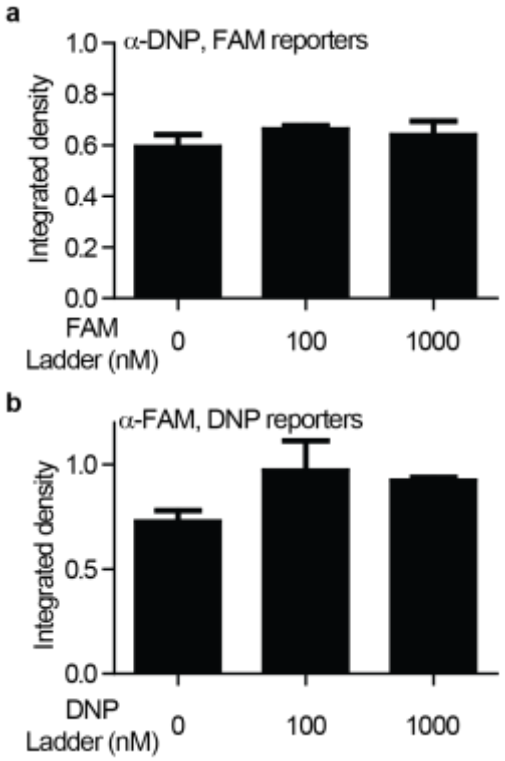

Supplementary Figure 10. Orthogonality of paper ELISA detection. (**a**) FAM reporters did not bind to the DNP paper ELISA (anti-DNP). (**b**) Similarly, DNP reporters did not react with the FAM paper ELISA (anti-FAM).

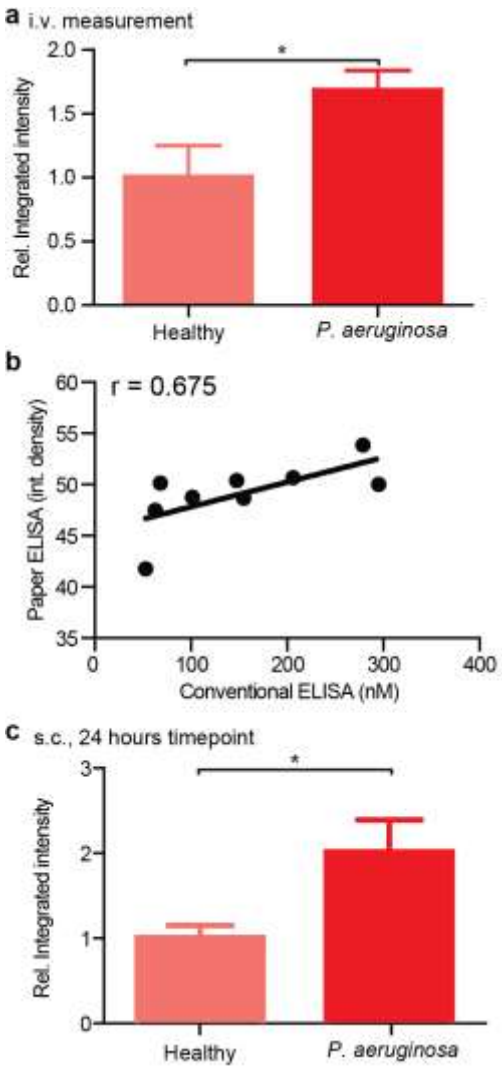

Supplementary Figure 11. DNP paper ELISA to quantify reporter concentration in urine. (**a**) Paper ELISA analysis matches signal from conventional ELISA (see Fig. 5b). (**b**) Correlation between signal from conventional ELISA and paper ELISA (Pearson's r = 0.675, P value: 0.0459). (**c**) Paper ELISA analysis of the 24-hour timepoint from s.c. experiment showing elevated urine signal from infected mice (see Fig. 5c).

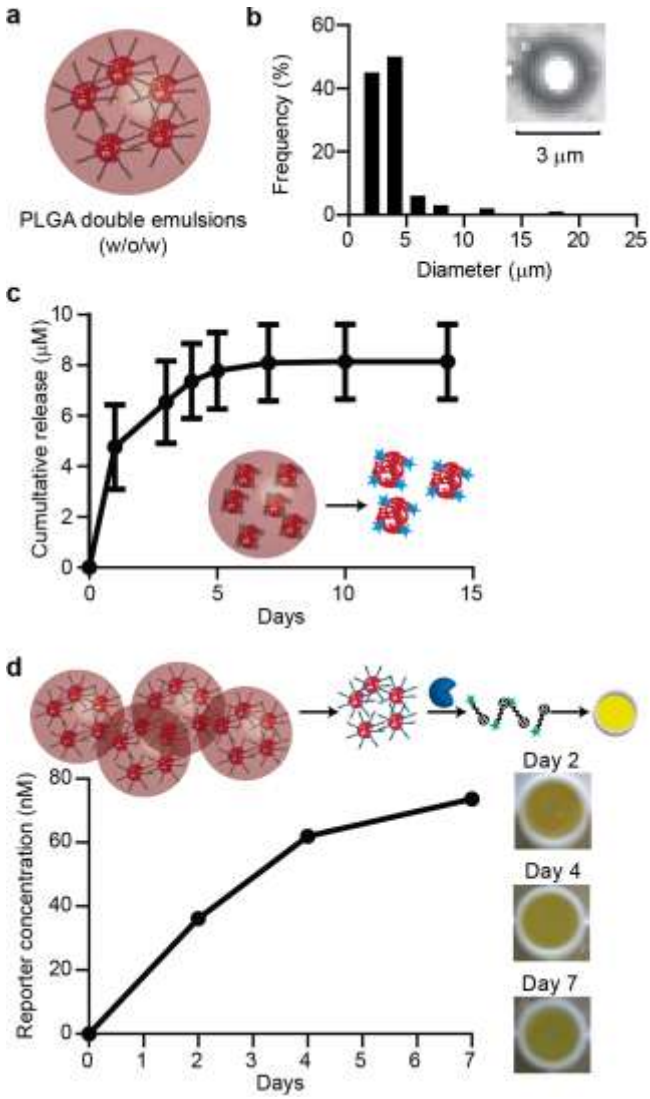

Supplementary Figure 12. Compatibility of PEG-chaperoned synthetic biomarkers with PLGA microspheres. (**a**) PEG-chaperoned particles were encapsulated in poly(lactide-*co*-glycolide) (PLGA) (50 lactide:50 glycolide) double emulsions that (**b**) formed small micron-sized microspheres. (**c**) Release kinetics of fluorescently labeled PEG from PLGA microspheres at 37 ºC. (**d**) PEG-T1E was encapsulated in PLGA microspheres. Released PEG-T1E was incubated with thrombin and released reporters were measured by ELISA and accumulated total reporter concentration calculated for each day.